ASYMPTOTICALLY MINIMUM BIT ERROR RATE BLOCK PRECODERS FOR MINIMUM MEAN SQUARE ERROR EQUALIZATION

Scarlett S. Chan, Timothy N. Davidson and K. Max Wong

McMaster University
Department of Electrical and Computer Engineering
Hamilton, Ontario, Canada, L8S 4K1

ABSTRACT

In this paper, we determine linear block precoders which asymptotically minimize the bit error rate (BER) of block-based communication systems employing minimum mean square error (MMSE) equalization and threshold detection. The problem is solved by a two-stage optimization procedure in which a lower bound on the BER over its convex region is first minimized, followed by showing that this lower bound is actually achieved by the solution obtained in the first stage. Simulation results show that at moderate-to-high signal-to-noise ratios (SNRs), the SNR gain for the proposed design over the standard MMSE precoder, and several other conventional systems such as orthogonal frequency division multiplexing (OFDM) and discrete multitone (DMT) modulation can be several decibels (dB).

1. INTRODUCTION

The reception of data transmitted serially over a dispersive medium is complicated by the presence of channel-induced intersymbol interference (ISI). Although many techniques for reducing the complexity of optimal reception have been proposed (e.g., decision feedback equalization), the receiver complexity can often be substantially reduced by transmitting the data in blocks. Common schemes that employ this technique include orthogonal frequency division multiplexing (OFDM) and discrete multitone (DMT) modulation, both of which employ linear block-by-block transmission and block-by-block reception. Recently, a rather general class of linear block-by-block transmission schemes has received considerable attention [1, 2]. In particular, linear block precoders which minimize the mean square error (MSE) of the equalized data have been determined for (linear) zero-forcing (ZF) and minimum mean square error (MMSE) equalization strategies [1]. Although these designs result in minimum MSE, they do not necessarily result in minimum bit error rate (BER). Following previous work on minimum BER precoders for ZF equalization [3, 4], we will derive herein linear block precoders for systems with (linear) MMSE equalizers and threshold detection which (asymptotically) minimize the BER as the size of the transmitted block grows.

2. BLOCK TRANSMISSION

The block-based transceiver model used in this paper is shown in Fig. 1. Special cases of this model can be used to describe OFDM, DMT, CDMA and TDMA transmission schemes [1]. In this model, within one time frame, a block of M data symbols, $\boldsymbol{s}(n)$, is processed by the precoder matrix, $\boldsymbol{F}_0$, so that a block of P data symbols, $\boldsymbol{u}(n)$, is transmitted over the channel. At the receiver, a block of M equalized data symbols, $\hat{\boldsymbol{s}}(n)$, is reconstructed from a received data symbol block, $\boldsymbol{r}(n)$. If M is greater than the order of the channel, L, and $P \geq M + L$, then the inter-block interference (IBI) in $\hat{\boldsymbol{s}}(n)$ is caused by the previous transmitted data block, $\boldsymbol{s}(n-1)$, only. By the use of zero-padded (ZP) or cyclic-prefixed (CP) transmission, this undesirable IBI can be eliminated. If we choose $P = M + L$, then, in ZP transmission, the precoder matrix is of the form $\boldsymbol{F}_0 = \left[\begin{smallmatrix}\boldsymbol{F}\\ \boldsymbol{0}\end{smallmatrix}\right]$, where $\boldsymbol{F}$ is $M \times M$, and the equalizer matrix $\boldsymbol{G}_0 = \boldsymbol{G}$ is $M \times P$, [1]. With the same choice of P, IBI is eliminated in the CP case by choosing $\boldsymbol{F}_0 = \begin{bmatrix}[\boldsymbol{0}, \boldsymbol{I}_L]\\ \boldsymbol{I}_M\end{bmatrix}\boldsymbol{F}$, and $\boldsymbol{G}_0 = [\boldsymbol{0}, \boldsymbol{G}]$, where $\boldsymbol{F}$ and $\boldsymbol{G}$ are both $M \times M$, [1]. In both schemes, the equalized signal can be expressed as

$$\hat{\boldsymbol{s}} = \boldsymbol{GHFs} + \boldsymbol{Gv}, \tag{1}$$

where $\boldsymbol{v}$ is a vector of additive noise samples at the receiver, and we have dropped the explicit dependence on the time index, n. In ZP schemes, $\boldsymbol{H}$ is a $P \times M$ tall Toeplitz matrix and in CP schemes $\boldsymbol{H}$ is an $M \times M$ circulant matrix. Throughout this paper, we assume that both transmitter and receiver have perfect knowledge of the channel, and the transmitted data are uncorrelated equiprobable four-phase quadrature amplitude modulation (4-QAM) symbols with $\mathrm{E}\{\boldsymbol{ss}^H\} = \boldsymbol{I}$. We also assume that the receiver noise is zero-mean, white, circular, and Gaussian with covariance matrix $\mathrm{E}\{\boldsymbol{vv}^H\} = \sigma^2\boldsymbol{I}$. The MMSE equalizer for this scenario is given by

$$\boldsymbol{G} = \boldsymbol{G}_{\mathrm{MMSE}} = \boldsymbol{F}^H\boldsymbol{H}^H(\sigma^2\boldsymbol{I} + \boldsymbol{HFF}^H\boldsymbol{H}^H)^{-1}. \tag{2}$$

For notational simplicity, we will set $\boldsymbol{G} = \boldsymbol{G}_{\mathrm{MMSE}}$ in the remaining parts of the paper.

3. AVERAGE BIT ERROR RATE

With threshold detection applied independently on the real and imaginary parts of each component of the received signal vector $\hat{\boldsymbol{s}}$ in Fig. 1, the detected signal can be written as

$$\hat{\boldsymbol{s}}_{\mathrm{q}} = \mathrm{sgn}\big(\mathrm{Re}(\hat{\boldsymbol{s}})\big) + j\mathrm{sgn}\big(\mathrm{Im}(\hat{\boldsymbol{s}})\big), \tag{3}$$

where $\mathrm{Re}(\cdot)$ and $\mathrm{Im}(\cdot)$ take the real and imaginary part of a complex vector, respectively, and $\mathrm{sgn}(\cdot)$ quantizes the elements in the signal vector to be ± 1. Similar to [3, 4], the average bit error rate,

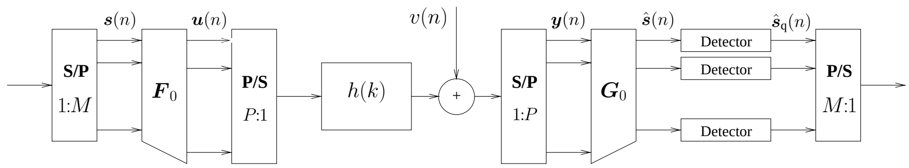

Fig. 1. Discrete-time baseband equivalent model of a block-based transceiver

P_{e}, is defined to be the average probability of receiving an erroneous bit in $\hat{\boldsymbol{s}}_{\text{q}}$. Therefore,

$$P_{\text{e}} = \frac{1}{2M} \sum_{m=1}^{M} (P_{\text{e,r},m} + P_{\text{e,i},m}), \tag{4}$$

where $P_{\text{e,r},m}$ and $P_{\text{e,i},m}$ represent the probability of error in the real and imaginary part of the mth element of the detected signal vector, respectively. Notice that (1) can be expressed in the form

$$\hat{\boldsymbol{s}} = \text{Diag}(\boldsymbol{GHF})\boldsymbol{s} + \big(\boldsymbol{GHF} - \text{Diag}(\boldsymbol{GHF})\big)\boldsymbol{s} + \boldsymbol{Gv} \tag{5}$$

so that the desired signal, ISI and noise terms are distinguished. Here, $\text{Diag}(\boldsymbol{GHF})$ is an $M \times M$ matrix with the diagonal elements of $\boldsymbol{GHF}$ on its diagonal, and zeros elsewhere. The probabilities $P_{\text{e,r},m}$ and $P_{\text{e,i},m}$ can be awkward to compute directly because they each involve a sum over the 4^{M-1} values which the other elements of $\boldsymbol{s}$ may take on. A standard approach to reduce the complexity of evaluating these expressions is to determine an approximate statistical model for the ISI in (5). To do so, we observe that single-user block transmission is algebraically equivalent to a class of (synchronous) multi-user serial transmission systems. In particular, the ISI in (5) is algebraically equivalent to the multiple-access interference (MAI) in the multi-user scenario. By transforming the results in [5, 6] on the MAI distribution at the output of a linear MMSE multi-user detector to the scenario in (5), it can be shown that for a randomly chosen channel $h(k)$ [of order L] and a randomly chosen $M \times M$ precoder $\boldsymbol{F}$, the distribution of the ISI in each element of $\hat{\boldsymbol{s}}$ in (5) converges almost surely to a Gaussian distribution as the block size, M, increases. Therefore, each element of $\hat{\boldsymbol{s}}$ in (5) can (almost surely) be approximated by a Gaussian random variable, and the accuracy of the approximation improves as M increases. If we let $[\cdot]_m$ denote the mth element of a vector and $[\cdot]_{\ell m}$ denote the (ℓ, m)th element of a matrix, then the real and imaginary parts of $\hat{\boldsymbol{s}}$ are approximated as

$$\big[\text{Re}(\hat{\boldsymbol{s}})\big]_m \approx \boldsymbol{x}_{\text{r},m} \sim \mathcal{N}\Big([\boldsymbol{GHF}]_{mm}\big[\text{Re}(\boldsymbol{s})\big]_m, [\boldsymbol{C}]_{mm}\Big), \tag{6}$$

$$\big[\text{Im}(\hat{\boldsymbol{s}})\big]_m \approx \boldsymbol{x}_{\text{i},m} \sim \mathcal{N}\Big([\boldsymbol{GHF}]_{mm}\big[\text{Im}(\boldsymbol{s})\big]_m, [\boldsymbol{C}]_{mm}\Big), \tag{7}$$

where $\boldsymbol{C}$ is the (covariance) matrix which satisfies

$$\begin{aligned} 2\boldsymbol{C} = &\big(\text{Re}(\boldsymbol{GHF}) - \text{Diag}(\boldsymbol{GHF})\big) \\ &\times \big(\text{Re}(\boldsymbol{GHF}) - \text{Diag}(\boldsymbol{GHF})\big)^T \\ &+ \big(\text{Im}(\boldsymbol{GHF})\big)\big(\text{Im}(\boldsymbol{GHF})\big)^T + \sigma^2 \text{Re}(\boldsymbol{GG}^H). \end{aligned} \tag{8}$$

By following standard procedures for calculating the probability of error in threshold detection of an antipodal symbol in Gaussian interference (e.g., [7]), and using (6) and (7), we have

$$P_{\text{e,r},m} = P_{\text{e,i},m} \approx \frac{1}{2}\text{erfc}\left(\frac{[\boldsymbol{GHF}]_{mm}}{\sqrt{4[\boldsymbol{C}]_{mm}}}\right), \tag{9}$$

where $\text{erfc}(x) = \frac{2}{\sqrt{\pi}} \int_x^\infty \exp(-z^2) dz$. An interesting property of the MMSE equalizer is that

$$(\boldsymbol{GHF})(\boldsymbol{GHF})^H + \sigma^2 \boldsymbol{GG}^H = \boldsymbol{GHF}. \tag{10}$$

Using (10), it can be shown that

$$2[\boldsymbol{C}]_{mm} = [\boldsymbol{GHF}]_{mm} - \big([\boldsymbol{GHF}]_{mm}\big)^2, \tag{11}$$

and hence that the right-hand side of (9) is equal to

$$\frac{1}{2}\text{erfc}\left(\left(2\Big[\big(\text{Diag}(\boldsymbol{GHF})\big)^{-1} - \boldsymbol{I}\Big]_{mm}\right)^{-1/2}\right). \tag{12}$$

By substituting (12) into (4), the average probability of error can be written as

$$P_{\text{e}} \approx \frac{1}{2M} \sum_{m=1}^{M} \text{erfc}\left(\left(2\Big[\big(\text{Diag}(\boldsymbol{GHF})\big)^{-1} - \boldsymbol{I}\Big]_{mm}\right)^{-1/2}\right), \tag{13}$$

where the approximation converges (almost surely) as the block size grows.

A key element of our design method is the following observation regarding the convexity in (13). Let $f(x) = \text{erfc}(\frac{1}{\sqrt{2x}})$ for some $x > 0$. Then,

$$\frac{d^2 f(x)}{dx^2} = \frac{1}{\sqrt{2\pi}} \exp\left(-\frac{1}{2x}\right) x^{-5/2} \left(\frac{1}{2x} - \frac{3}{2}\right). \tag{14}$$

From (14), if $x > \frac{1}{3}$, then $\frac{d^2 f(x)}{dx^2} > 0$. Therefore, P_{e} is a convex function of $\Big[\big(\text{Diag}(\boldsymbol{GHF})\big)^{-1} - \boldsymbol{I}\Big]_{mm}$ if

$$[\boldsymbol{GHF}]_{mm} \geq \frac{3}{4} \quad \forall m \in [1, M]. \tag{15}$$

4. DESIGN OF MINIMUM BER PRECODER

Using the asymptotic BER expression in (13), we would like to find a precoder which provides minimum BER, subject to an upper bound on the (average) power used to transmit the data. Therefore, the design problem for both ZP and CP systems can be written as

$$\begin{aligned} \min_{\boldsymbol{F}} \quad & P_{\text{e}} \\ \text{subject to} \quad & \text{tr}(\boldsymbol{FF}^H) \leq p_0. \end{aligned} \tag{16}$$

To ensure that the solution is globally optimal, only the convex region of the BER is under consideration. Within the convex region, we can use the Jensen's Inequality [8] to obtain the following lower bound on the BER,

$$P_{\text{e}} \geq \frac{1}{2}\text{erfc}\left(\frac{2}{M}\sum_{m=1}^{M}\left(\Big[\big(\text{Diag}(\boldsymbol{GHF})\big)^{-1} - \boldsymbol{I}\Big]_{mm}\right)^{-1/2}\right)$$

$$= \frac{1}{2}\text{erfc}\left(\left(\frac{2}{M}\left(\text{tr}\left(\left(\text{Diag}(\boldsymbol{GHF})\right)^{-1}\right) - M\right)\right)^{-1/2}\right)$$
$$\triangleq P_{\text{e,LB}}, \tag{17}$$

where equality holds if and only if $[\boldsymbol{GHF}]_{mm}$ are the same for all $m \in [1, M]$. To solve (16) in the region in which P_{e} is convex, we first minimize $P_{\text{e,LB}}$ subject to the transmitter power and convexity constraints, and then show that the minimized lower bound is achievable. As $\text{erfc}(\cdot)$ is a monotonically decreasing function, minimizing the lower bound on $P_{\text{e,LB}}$ is equivalent to minimizing $\text{tr}\Big(\big(\text{Diag}(\boldsymbol{GHF})\big)^{-1}\Big)$. For convenience, we parameterize $\boldsymbol{F} = \boldsymbol{V\Phi U}^H$ in terms of its singular value decomposition, and write the eigenvalue decomposition of $(\boldsymbol{H}^H\boldsymbol{H})^{-1}$ as $\boldsymbol{W\Lambda W}^H$, where the columns in $\boldsymbol{W}$ are arranged in such a way that λ_{ii}, the diagonal elements of $\boldsymbol{\Lambda}$, are in descending order. The design problem in (16) in the region in which P_{e} is convex can then be written as

$$\min_{\boldsymbol{V},\boldsymbol{\Phi},\boldsymbol{U}} \quad \text{tr}\left(\left(\text{Diag}\big(\boldsymbol{U\Gamma U}^H\big)\right)^{-1}\right) \tag{18a}$$
$$\text{subject to} \quad \text{tr}(\boldsymbol{\Phi}^2) \le p_0, \tag{18b}$$
$$\big[\boldsymbol{U\Gamma U}^H\big]_{mm} \ge \frac{3}{4} \qquad \forall m \in [1, M], \tag{18c}$$

where $\boldsymbol{\Gamma} = (\sigma^2\boldsymbol{\Phi}^{-1}\boldsymbol{V}_1\boldsymbol{\Lambda}\boldsymbol{V}_1{}^H\boldsymbol{\Phi}^{-1} + \boldsymbol{I})^{-1}$, and $\boldsymbol{V}_1 = \boldsymbol{V}^H\boldsymbol{W}$.

Problem (18) is awkward to solve directly due to the constraint (18c). Therefore, we will solve (18) by first dealing with (18c) for any given $\boldsymbol{\Gamma}$ and then solve the remaining problem. This may appear to be difficult at first, because $\boldsymbol{U}$ appears in both (18a) and (18c). A key observation that we will make below is that, for a fixed $\boldsymbol{\Gamma}$, the $\boldsymbol{U}$ which maximizes the minimum satisfaction of the constraint in (18c) (or minimizes the maximum constraint violation) also minimizes the objective in (18a). To facilitate the derivation, let $\boldsymbol{\Gamma} = \boldsymbol{X}\tilde{\boldsymbol{\Gamma}}\boldsymbol{X}^H$ denote the eigenvalue decomposition of $\boldsymbol{\Gamma}$. By modifying Lemma 1 of [3, 4], it can be shown that, for a fixed $\boldsymbol{\Gamma}$

$$\max_{\boldsymbol{UU}^H=\boldsymbol{I}} \quad \min_{m} \, [\boldsymbol{U\Gamma U}^H]_{mm} = \text{tr}(\boldsymbol{\Gamma})/M. \tag{19}$$

Moreover, the maximum in (19) can be achieved by choosing $\boldsymbol{U} = \boldsymbol{DX}^H$, where $\boldsymbol{D}$ is a normalized $M \times M$ Discrete Fourier Transform (DFT) matrix. (The result remains valid if we replace $\boldsymbol{D}$ by $\boldsymbol{D}^H$, the corresponding normalized inverse DFT matrix.) Therefore, if $\text{tr}(\boldsymbol{\Gamma})/M \ge 3/4$, then $\boldsymbol{U} = \boldsymbol{DX}^H$ is a feasible choice in (18). Otherwise, the feasible set of (18c) is empty, and hence (18) has no solution. We will now show that $\boldsymbol{DX}^H$ is in fact an optimal choice for $\boldsymbol{U}$ in (18).

To do so we consider the following relaxed version of (18): minimize (18a) subject to (18b) in the absence of (18c). Since the power constraint does not depend on $\boldsymbol{U}$, for a fixed $\boldsymbol{\Gamma}$, we can find an optimal $\boldsymbol{U}$ for the relaxed problem, denoted by $\boldsymbol{U}_{\text{rel},\boldsymbol{\Gamma}}$, by solving

$$\min_{\boldsymbol{UU}^H=\boldsymbol{I}} \text{tr}\Big(\big(\text{Diag}(\boldsymbol{U\Gamma U}^H)\big)^{-1}\Big). \tag{20}$$

Since $\boldsymbol{\Gamma}$ is positive definite, we can apply the arithmetic-geometric mean inequality [9] to show that

$$\text{tr}\Big(\big(\text{Diag}(\boldsymbol{U\Gamma U}^H)\big)^{-1}\Big) \ge \frac{M}{\big(\Pi_{m=1}^M[\boldsymbol{U\Gamma U}^H]_{mm}\big)^{1/M}}. \tag{21}$$

Applying the arithmetic-geometric mean inequality again we have

$$\big(\Pi_{m=1}^M[\boldsymbol{U\Gamma U}^H]_{mm}\big)^{1/M} \le \frac{1}{M}\sum_{m=1}^M[\boldsymbol{U\Gamma U}^H]_{mm}, \tag{22}$$

and hence

$$\text{tr}\Big(\big(\text{Diag}(\boldsymbol{U\Gamma U}^H)\big)^{-1}\Big) \ge M^2/\text{tr}(\boldsymbol{\Gamma}). \tag{23}$$

The inequalities in (21) and (22), and hence that in (23) hold with equality if the diagonal elements of $\boldsymbol{U\Gamma U}^H$ are all equal. Now, define $\boldsymbol{U}_1 = \boldsymbol{DX}^H$, where, as above, $\boldsymbol{\Gamma} = \boldsymbol{X}\tilde{\boldsymbol{\Gamma}}\boldsymbol{X}^H$ is the eigenvalue decomposition of $\boldsymbol{\Gamma}$. Then $\boldsymbol{U}_1\boldsymbol{\Gamma}\boldsymbol{U}_1^H = \boldsymbol{D}\tilde{\boldsymbol{\Gamma}}\boldsymbol{D}^H$, which implies that $[\boldsymbol{U}_1\boldsymbol{\Gamma}\boldsymbol{U}_1^H]_{mm} = \text{tr}(\tilde{\boldsymbol{\Gamma}})/M$, because the magnitude of each element of $\boldsymbol{D}$ is $1/\sqrt{M}$. Therefore, $\boldsymbol{U} = \boldsymbol{U}_1$ achieves the lower bound in (23); i.e.,

$$\text{tr}\Big(\big(\text{Diag}(\boldsymbol{U}_1\boldsymbol{\Gamma}\boldsymbol{U}_1^H)\big)^{-1}\Big) = M^2/\text{tr}(\boldsymbol{\Gamma}). \tag{24}$$

Hence, an optimal solution to (20) is $\boldsymbol{U}_{\text{rel},\boldsymbol{\Gamma}} = \boldsymbol{U}_1 = \boldsymbol{DX}^H$. As shown in the previous paragraph, if the additional constraint (18c) is satisfiable for the given $\boldsymbol{\Gamma}$, then $\boldsymbol{U}_1$ is in the feasible set. Therefore, for a fixed $\boldsymbol{\Gamma}$, (i.e., fixed $\boldsymbol{\Phi}$ and $\boldsymbol{V}$), an optimal choice of $\boldsymbol{U}$ in (18) is $\boldsymbol{U}_{\text{opt},\boldsymbol{\Gamma}} = \boldsymbol{U}_{\text{rel},\boldsymbol{\Gamma}} = \boldsymbol{DX}^H$.

Now that we have found the optimal $\boldsymbol{U}$, what remains to be done is to find the $\boldsymbol{\Phi}$ and $\boldsymbol{V}$ which solve

$$\min_{\boldsymbol{\Phi},\boldsymbol{V}} \quad \text{tr}\left(\left(\text{Diag}\big(\boldsymbol{U}_{\text{opt},\boldsymbol{\Gamma}}\boldsymbol{\Gamma}\boldsymbol{U}_{\text{opt},\boldsymbol{\Gamma}}^H\big)\right)^{-1}\right) \tag{25a}$$
$$\text{subject to} \quad \text{tr}(\boldsymbol{\Phi}^2) \le p_0. \tag{25b}$$

Since $\big([\boldsymbol{U}_{\text{opt},\boldsymbol{\Gamma}}\boldsymbol{\Gamma}\boldsymbol{U}_{\text{opt},\boldsymbol{\Gamma}}^H]_{mm}\big)^{-1} = M/\text{tr}(\boldsymbol{\Gamma})$, minimizing (25a) is equivalent to maximizing $\text{tr}(\boldsymbol{\Gamma})$, which is, in turn, equivalent to minimizing $-\text{tr}(\boldsymbol{\Gamma})$. Now the mean square error of the equalized symbols, $\text{E}\Big\{\sum_{m=1}^M\big([\hat{\boldsymbol{s}}]_m - [\boldsymbol{s}]_m\big)^2\Big\}$, is given by

$$\text{MSE} = \text{tr}\big((\boldsymbol{GHF}-\boldsymbol{I})(\boldsymbol{GHF}-\boldsymbol{I})^H + \sigma^2\boldsymbol{GG}^H\big). \tag{26}$$

Using (10) and some properties of the trace function, we have $\text{MSE} = \text{tr}(\boldsymbol{I} - \boldsymbol{\Gamma}^H)$ and hence minimizing $-\text{tr}(\boldsymbol{\Gamma})$ is equivalent to minimizing the MSE. Therefore, the $\boldsymbol{\Phi}$ and $\boldsymbol{V}$ which solve (25) are those which minimize the MSE of the equalized symbols. Before we exploit that fact we recall that $(\boldsymbol{H}^H\boldsymbol{H})^{-1} = \boldsymbol{W\Lambda W}$ denotes the eigenvalue decomposition of $(\boldsymbol{H}^H\boldsymbol{H})^{-1}$ with the diagonal elements of $\boldsymbol{\Lambda}$ in descending order. If the signal-to-noise ratio (SNR), $\rho = \frac{p_0}{P\sigma^2}$, satisfies

$$\rho \ge \frac{1}{P}\big(\text{tr}(\boldsymbol{\Lambda}^{1/2})\sqrt{\lambda_{11}} - \text{tr}(\boldsymbol{\Lambda})\big), \tag{27}$$

then the $\boldsymbol{V}$ and $\boldsymbol{\Phi}$ which solve (25) are [1, 10]

$$\boldsymbol{V}_{\text{MMSE}} = \boldsymbol{W}, \tag{28a}$$
$$[\boldsymbol{\Phi}_{\text{MMSE}}]_{mm} = \left(\frac{p_0 + \sigma^2\text{tr}(\boldsymbol{\Lambda})}{\text{tr}(\boldsymbol{\Lambda}^{1/2})}\sqrt{\lambda_{mm}} - \sigma^2\lambda_{mm}\right)^{1/2}. \tag{28b}$$

[The case of SNRs which do not satisfy (27) will be dealt with in the next section.] In order for $\boldsymbol{V}_{\text{MMSE}}$ in (28) to constitute a feasible solution to the original problem in (18) we require that

$$\text{tr}(\boldsymbol{\Gamma})/M \ge 3/4 \tag{29}$$

so that there exists a $\boldsymbol{U}$ which satisfy (18c). (If this condition is satisfied then $\boldsymbol{U} = \boldsymbol{U}_{\text{opt},\boldsymbol{\Gamma}} = \boldsymbol{D}\boldsymbol{X}^H$ will suffice.) By substituting (28) into (29) we determine that (29) holds for SNRs satisfying

$$\rho \geq \frac{1}{P}\left(\frac{4\big(\mathrm{tr}(\boldsymbol{\Lambda}^{1/2})\big)^2}{M} - \mathrm{tr}(\boldsymbol{\Lambda})\right). \quad (30)$$

Therefore, if the SNR satisfies the bounds in (27) and (30) then a precoder which minimizes the lower bound on the probability of error is $\boldsymbol{F}_{\text{min, LB}} = \boldsymbol{W}\boldsymbol{\Phi}_{\text{MMSE}}\boldsymbol{U}_{\text{opt},\boldsymbol{\Gamma}}$, where $\boldsymbol{U}_{\text{opt},\boldsymbol{\Gamma}} = \boldsymbol{D}$ because $\boldsymbol{\Gamma}$ is diagonal in this case. An important property of $\boldsymbol{F}_{\text{min, LB}}$ is that the resulting diagonal elements of $\boldsymbol{G}\boldsymbol{H}\boldsymbol{F}$ are all equal. Therefore, $\boldsymbol{F}_{\text{min, LB}}$ not only minimizes the lower bound on the probability of error, but also achieves the lower bound. That is, for SNRs which satisfy (27) and (30), a precoder which (asymptotically) minimizes the BER is

$$\boldsymbol{F}_{\text{MBER}} = \boldsymbol{W}\boldsymbol{\Phi}_{\text{MMSE}}\boldsymbol{D}. \quad (31)$$

For comparison, the set of all MMSE precoders is of the form [1]

$$\boldsymbol{F}_{\text{MMSE}} = \boldsymbol{W}\boldsymbol{\Phi}_{\text{MMSE}}\tilde{\boldsymbol{U}}, \quad (32)$$

where $\tilde{\boldsymbol{U}}$ is an arbitrary unitary matrix. Comparing (31) and (32), it is clear that our minimum BER precoder is an MMSE precoder with a specially chosen unitary matrix. That is, the minimum BER precoder also minimizes the MSE, but an arbitrary MMSE precoder does not necessarily minimize the BER.

5. SUB-CHANNEL DROPPING SCHEME

The minimum BER precoder derived in Section 4 is valid if the SNR satisfies

$$\rho \geq \rho_c \triangleq \frac{1}{P}\left(\max\Big\{\frac{4\big(\mathrm{tr}(\boldsymbol{\Lambda}^{1/2})\big)^2}{M} - \mathrm{tr}(\boldsymbol{\Lambda}), \mathrm{tr}(\boldsymbol{\Lambda}^{1/2})\sqrt{\lambda_{11}} - \mathrm{tr}(\boldsymbol{\Lambda})\Big\}\right). \quad (33)$$

This SNR threshold is a function of the channel impulse response and the block size, M, only, and can be computed without having to compute the minimum BER precoder itself. The threshold guarantees the minimized lower bound in (18) is valid (i.e., the BER expression in (13) is in its convex region), and the elements of $\boldsymbol{\Phi}_{\text{MMSE}}$ are non-negative. In cases where $\rho < \rho_c$ and in systems in which the transmitter power cannot be increased, we can reduce the threshold by closing some low-gain subchannels (and hence reducing the block size), and re-allocating the transmitter power to the surviving channels [11, 4, 3, 10]. Once the threshold has been sufficiently reduced, we can obtain a minimum BER precoder for the reduced system using a variation of (31) as we now outline:

1. Let $\bar{M} = M$, and $\bar{\boldsymbol{\Lambda}} = \boldsymbol{\Lambda}$.
2. Determine the reduced block size $\bar{M}$: Calculate $\bar{\rho}_c$ using (33) with M and $\boldsymbol{\Lambda}$ replaced by $\bar{M}$ and $\bar{\boldsymbol{\Lambda}}$, respectively. While $\rho < \bar{\rho}_c$, decrease $\bar{M}$ by 1, and set the first non-zero diagonal elements of $\bar{\boldsymbol{\Lambda}}$ to zero.
3. Construct $\bar{\boldsymbol{\Phi}}_{\text{MMSE}}$ using (28b) with $\boldsymbol{\Lambda}$ replaced by $\bar{\boldsymbol{\Lambda}}$, and let $\bar{\boldsymbol{W}}$ denotes the last $\bar{M}$ columns of $\boldsymbol{W}$.
4. The minimum BER precoder for the reduced system is then
$$\bar{\boldsymbol{F}}_{\text{MBER}} = \bar{\boldsymbol{W}}\bar{\boldsymbol{\Phi}}_{\text{MMSE}}\bar{\boldsymbol{D}}, \quad (34)$$
where $\bar{\boldsymbol{D}}$ is a normalized $\bar{M} \times \bar{M}$ DFT matrix (or IDFT matrix).

6. MBER PRECODERS FOR CP SYSTEMS

As indicated in Section 2, inter-block interference can be eliminated by zero-padding (ZP) or cyclic-prefix (CP) transmission schemes. By constructing the channel matrix $\boldsymbol{H}$ differently, the output data symbol block for both schemes can be described by (1). In CP schemes, as $\boldsymbol{H}$ is circulant, the expression for the minimum BER precoder can be simplified. For CP schemes, we have

$$\boldsymbol{H} = \boldsymbol{H}_{cp} = \boldsymbol{D}^H\boldsymbol{\Delta}\boldsymbol{D}, \quad (35)$$

where $\boldsymbol{D}$ is a normalized DFT matrix of size M, and $\boldsymbol{\Delta}$ is an $M \times M$ diagonal matrix with ith diagonal element

$$[\boldsymbol{\Delta}]_{ii} = H(e^{j2\pi(i-1)/M}) = \sum_n h(n)e^{-j2\pi(i-1)n/M}. \quad (36)$$

As the minimum BER precoder proposed in Section 4 is also applicable for CP systems, the minimum BER precoder for CP systems can be written as

$$\boldsymbol{F}_{\text{CP-MBER}} = \boldsymbol{D}^H\boldsymbol{P}^T\boldsymbol{\Phi}_{\text{MMSE}}\boldsymbol{D}, \quad (37)$$

where $\boldsymbol{P}$ is the permutation matrix that arranges the diagonal elements of $(\boldsymbol{\Delta}^H\boldsymbol{\Delta})^{-1}$ in descending order for the convenience of sub-channel dropping, and the corresponding $\boldsymbol{\Lambda}$ in (28b) is $\boldsymbol{P}^T(\boldsymbol{\Delta}^H\boldsymbol{\Delta})^{-1}\boldsymbol{P}$. As indicated in (37), the CP-MBER precoder has a similar structure to the standard DMT precoder except that the diagonal power loading matrix of DMT is replaced by the MMSE power loading matrix post-multiplied by a DFT matrix.

7. SIMULATION RESULTS

In this section, the theoretical and simulated BER performance for various ZP and CP schemes at different SNRs are evaluated for a third-order FIR channel with zeros at $0.7, 0.5\exp(j2\pi 0.256)$ and $0.3\exp(j2\pi 0.141)$. The transmitter power, p_0, is fixed at 1. The block size $M = 32$ and the transmitted block size is $P = 35$. In Figs 2, 3 and 4, the theoretical BER is indicated by a solid line, and the simulated BER is represented by symbols. In Fig. 2, the theoretical and simulated BER performance of the proposed ZP minimum BER precoder is compared with the MMSE [1] precoder, the identity precoder with zero-padding (denoted by ZP-TDMA), and ZP-OFDM [1] designs. In Fig. 3, the BER performance of systems with the CP minimum BER precoder, MMSE, and conventional OFDM is presented. (The free unitary matrix in both the ZP and CP MMSE precoders is chosen to be the identity matrix.) The minimum SNR required to ensure the validity of our minimum BER solution before dropping any subchannels is $\max\{10.21\text{dB}, 6.65\text{dB}\}$ for the ZP case, and $\max\{10.48\text{dB}, 6.60\text{dB}\}$ in the CP case, where we have indicated both thresholds in (33). Therefore, no subchannels dropping has been performed for Figs 2 and 3. Fig. 4 shows the performance of systems employing ZP and CP minimum BER precoders and the conventional water-filling DMT system with subchannels dropping at low SNRs. In general, when the block sizes are the same, the ZP minimum BER precoder outperforms the CP minimum BER precoder by a small amount. (In fact, the improvement is slightly larger than shown, as the power used to transmit the cyclic-prefix is ignored in our SNR definition.) However, ZP minimum BER precoders are more complicated to implement, as they require the calculation of the eigen-vectors for different channels. In contrast, for the CP minimum BER precoders, the eigen-vector matrix is simply the normalized IDFT matrix (35), irrespective of the channel coefficients.

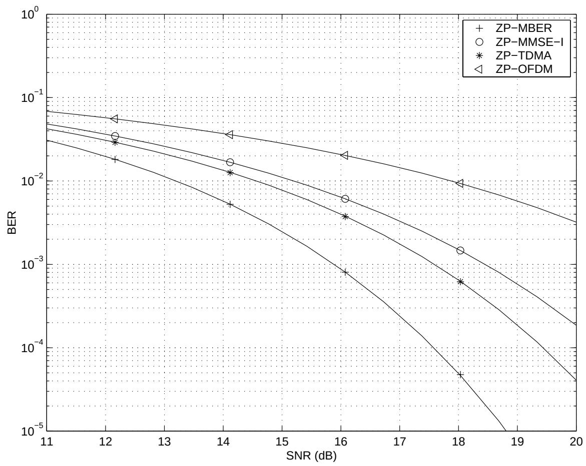

Fig. 2. ZP Precoders

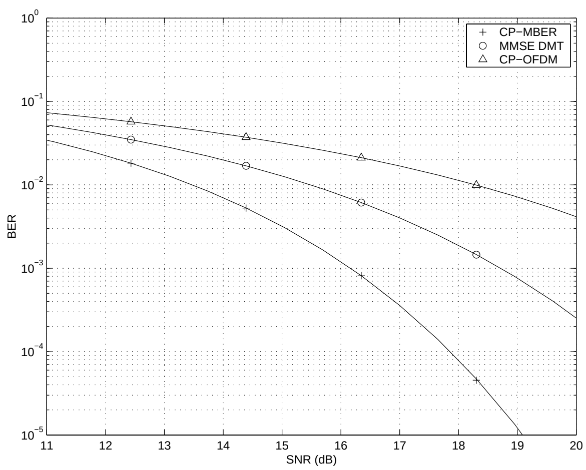

Fig. 3. CP Precoders

8. CONCLUSION

In this paper, linear precoders which minimize the asymptotic bit error rate (BER) were derived for block-based communication systems employing minimum mean square error equalization and threshold detection. Analytic solutions for the minimum BER precoder were obtained for two conventional schemes to remove interblock interference, namely, zero-padding and cyclic-prefix. These solutions were valid at (moderate-to-high) SNRs above a threshold which is dependent only on the channel impulse response and the block size. Simulation results showed that the asymptotic BER expression was quite close to the simulated BER, and that the SNR gain for the proposed minimum BER precoders over the conventional discrete multitone modulation and orthogonal frequency division multiplexing systems could be of the order of several decibels.

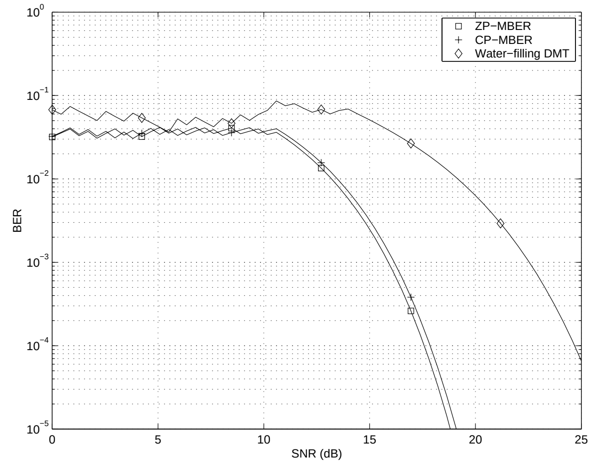

Fig. 4. CP and ZP Precoders with subchannels dropping

9. REFERENCES

[1] A. Scaglione, G. B. Giannakis, and S. Barbarossa, "Redundant filterbank precoders and equalizers Part 1: Unification and optimal designs," *IEEE Trans. Signal Processing*, vol. 47, no. 7, pp. 1988–2006, July 1999.

[2] A. Scaglione, S. Barbarossa, and G. B. Giannakis, "Filterbank transceivers optimizing information rate in block transmissions over dispersive channels," *IEEE Trans. Inform. Theory*, vol. 45, no. 3, pp. 1019–1032, April 1999.

[3] Y. W. Ding, T. N. Davidson, J. Zhang, Z. Q. Luo, and K. M. Wong, "Minimum BER block precoders for zero-forcing equalization," *Proc. Int. Conf. Acoust., Speech, Signal Processing*, May 2002.

[4] Y. W. Ding, T. N. Davidson, Z. Q. Luo, and K. M. Wong, "Minimum BER block precoders for zero-forcing equalization," Apr. 2002, Submitted to the *IEEE Trans. Signal Processing*.

[5] H. V. Poor and S. Verdú, "Probability of error in MMSE multiuser detection," *IEEE Trans. Inform. Theory*, vol. 43, no. 3, pp. 858–871, May 1997.

[6] J. Zhang, E. K. P. Chong, and D. N. C. Tse, "Output MAI distributions of linear MMSE multiuser receivers in DS-CDMA systems," *IEEE Trans. Inform. Theory*, vol. 47, no. 3, pp. 1128–1144, March 2001.

[7] J. G. Proakis, *Digital Communications*, McGraw Hill, fourth edition, 2001.

[8] T. M. Cover and J. A. Thomas, *Elements of Information Theory*, Wiley, 1991.

[9] R. A. Horn and C. R. Johnson, *Matrix Analysis*, Cambridge University Press, 1990.

[10] A. Scaglione, P. Stoica, S. Barbarossa, G. B. Giannakis, and H. Sampath, "Optimal designs for space-time linear precoders and decoders," *IEEE Trans. Signal Processing*, vol. 50, no. 5, pp. 1051–1064, May 2002.

[11] J. S. Chow, J. C. Tu, and J. M. Cioffi, "A discrete multitone transceiver system for HDSL applications," *IEEE J. Select. Areas Commun.*, vol. 9, no. 6, pp. 895–908, August 1991.